

Unscented Kalman filter with nonlinear dynamic process modeling for GPS navigation

Dah-Jing Jwo · Chun-Nan Lai

Received: 9 July 2007 / Accepted: 29 October 2007 / Published online: 24 November 2007
© Springer-Verlag 2007

Abstract This paper preliminarily investigates the application of unscented Kalman filter (UKF) approach with nonlinear dynamic process modeling for Global positioning system (GPS) navigation processing. Many estimation problems, including the GPS navigation, are actually nonlinear. Although it has been common that additional fictitious process noise can be added to the system model, however, the more suitable cure for non convergence caused by unmodeled states is to correct the model. For the nonlinear estimation problem, alternatives for the classical model-based extended Kalman filter (EKF) can be employed. The UKF is a nonlinear distribution approximation method, which uses a finite number of sigma points to propagate the probability of state distribution through the nonlinear dynamics of system. The UKF exhibits superior performance when compared with EKF since the series approximations in the EKF algorithm can lead to poor representations of the nonlinear functions and probability distributions of interest. GPS navigation processing using the proposed approach will be conducted to validate the effectiveness of the proposed strategy. The performance of the UKF with nonlinear dynamic process model will be assessed and compared to those of conventional EKF.

Keywords Extended Kalman filter · Unscented Kalman filter · Nonlinear model · Global positioning system (GPS)

Introduction

The Global positioning system (GPS) is a satellite-based navigation system that provides access to accurate positioning information anywhere on the globe. The extended Kalman filter (EKF) (Brown and Hwang 1997; Farrell and Barth 1999; Gelb 1974; Simon 2006) has been one of the promising approaches while employed in the GPS receiver as the navigational state estimator. The EKF not only works well in practice, but also it is theoretically attractive since it has been shown that it is the state estimator that minimizes the variance of the estimation mean square error (MSE). Nevertheless, the divergence due to modeling errors has been a critical problem in Kalman filter applications. The fact that EKF highly depends on a predefined dynamics model forms a major drawback. To achieve good filtering results, the designers are required to have the complete a priori knowledge on both the dynamic process and measurement models, in addition to the assumption that both the process and measurement are corrupted by zero-mean Gaussian white sequences. If the theoretical behavior of a filter and its actual behavior do not agree, divergence may occur.

Recently, there has been an increasing interest in the development of techniques for nonlinear estimation (Simon 2006; Gordon et al. 1993; Julier et al. 1995; Julier and Uhlmann 1997; Norgaard and Poulsen 2000; Wan and van der Merwe 2000), which can approximate the statistics of the process as accurately as possible. The process of state estimation combines a priori knowledge about the state and its transition due to a set of inputs, with a sequence of measurements. In general, the state estimate is recursively obtained in two stages: (1) the prediction and (2) the update. The well known optimal state estimator utilizes the analytical probability density function (PDF) to predict the states

D.-J. Jwo (✉) · C.-N. Lai
Department of Communications,
Navigation and Control Engineering,
National Taiwan Ocean University,
2 Peining Rd., Keelung 202-24, Taiwan
e-mail: djjwo@mail.ntou.edu.tw

using the total probability theorem and subsequently uses the measurement to update with Bayes’ rule. This optimal estimator requires storing the PDF and integrating it, and often results in impractical algorithms, therefore, techniques have been developed to approximate the optimal estimator.

Algorithms such as the EKF and unscented Kalman filter (UKF) (Wan and van der Merwe 2000; Wan and van der Merwe 2001) etc., focus on approximating the prediction probability characteristics and use the standard minimum MSE estimator. The EKF uses first order Taylor series expansion, which can be improved by higher order approximations at the expense of computational burden. The UKF has been developed in the context of state estimation of dynamic systems as a nonlinear distribution (or densities in the continuous case) approximation method. The UKF is superior to EKF not only in theory but in many practical situations. The algorithm uses a finite number of sigma points to propagate the probability of state distribution through the nonlinear dynamics of system. The algorithm performs the prediction of the statistics with a set of carefully chosen sample points for capturing mean and covariance of the system (Julier et al. 2000; Julier and Uhlmann 2002; Julier 2002). The UKF can capture the states up to at least second order, while the EKF is only a first order approximation.

The EKF has difficulty to ensure error convergence due to limited knowledge of the system’s dynamic model and measurement noise. If the Kalman filter is provided with information that the process behaves a certain way, whereas, it actually behaves a different way, the filter will continually intend to fit an incorrect process signal and the EKF estimates may not be reliable. In a number of practical situations, the availability of a precisely known model is unrealistic, which results in filtering performance degradation. Investigation of the nonlinear filtering approach to the navigation problem has been seen, but not as common as the EKF in the literature (van der Merwe and Wan 2004; Crassidis 2006; Li et al. 2006). In the actual GPS navigation filter design, there exists model uncertainties which cannot be expressed by the linear state-space model. It is very often the case that little a priori knowledge is available concerning the maneuver. In the modeling strategy, some phenomena are disregarded and a way to take them into account is to consider a nominal model affected by uncertainty. The linear model increases modeling errors since the actual vehicle motions are nonlinear process. Even it has been common that additional fictitious process noise can be added to the system model, nevertheless, the more suitable cure for non convergence caused by unmodeled states should be to correct the model.

This paper is organized in six sections. In Sect. 2, preliminary background on the extended Kalman filter for GPS navigation processing is briefly reviewed. The UKF is introduced in Sect. 3. Section 4 presents the GPS nonlinear

dynamic modeling. In Sect. 5, simulation experiment and analysis are carried out to evaluate the performance of the approach in comparison to those by conventional approach. Conclusions are given in Sect. 6.

The extended Kalman filter for GPS navigation processing

Kalman filtering has been recognised as one of the most powerful state estimation techniques. The purpose of the Kalman filter is to provide the estimation with minimum error variance. The extended Kalman filter is a nonlinear version of the Kalman filter and is widely used for the position estimation in GPS receivers. A superior way of solving the GPS navigation solution is to use the extended Kalman filter.

The extended Kalman filtering is a nonlinear version of Kalman filtering, which deals with the case governed by the nonlinear stochastic differential equations:

$$\dot{\mathbf{x}} = \mathbf{f}(\mathbf{x}, t) + \mathbf{u}(t) \tag{1a}$$

$$\mathbf{z} = \mathbf{h}(\mathbf{x}, t) + \mathbf{v}(t) \tag{1b}$$

where the vectors $\mathbf{u}(t)$ and $\mathbf{v}(t)$ are both white noise sequences with zero means and mutually independent:

$$\begin{aligned} E[\mathbf{u}(t)\mathbf{u}^T(\tau)] &= q\delta(t - \tau); \quad E[\mathbf{v}(t)\mathbf{v}^T(\tau)] = r\delta(t - \tau); \\ E[\mathbf{u}(t)\mathbf{v}^T(\tau)] &= \mathbf{0} \end{aligned} \tag{2}$$

where $\delta(t)$ is the Dirac delta function, $E[\cdot]$ represents expectation, and superscript “T” denotes matrix transpose.

Expressing Eqs. (1a) and (1b) in discrete-time equivalent form leads to

$$\mathbf{x}_{k+1} = \mathbf{f}_k(\mathbf{x}_k) + \mathbf{w}_k \tag{3a}$$

$$\mathbf{z}_k = \mathbf{h}_k(\mathbf{x}_k) + \mathbf{v}_k \tag{3b}$$

where the state vector $\mathbf{x}_k \in \mathcal{R}^n$, process noise vector $\mathbf{w}_k \in \mathcal{R}^n$, measurement vector $\mathbf{z}_k \in \mathcal{R}^m$, and measurement noise vector $\mathbf{v}_k \in \mathcal{R}^m$. In Eq. (3a, b), both the vectors \mathbf{w}_k and \mathbf{v}_k are zero mean Gaussian white sequences having zero crosscorrelation with each other:

$$\mathbf{E}[\mathbf{w}_k\mathbf{w}_i^T] = \begin{cases} \mathbf{Q}_k, & i = k \\ 0, & i \neq k \end{cases}; \quad \mathbf{E}[\mathbf{v}_k\mathbf{v}_i^T] = \begin{cases} \mathbf{R}_k, & i = k \\ 0, & i \neq k \end{cases}; \tag{4}$$

$$\mathbf{E}[\mathbf{w}_k\mathbf{v}_i^T] = \mathbf{0} \quad \text{for all } i \text{ and } k$$

where \mathbf{Q}_k is the process noise covariance matrix, \mathbf{R}_k is the measurement noise covariance matrix, and Δt is the sampling interval.

The discrete-time extended Kalman filter algorithm for the GPS navigation processing is summarized as follow:

1. Initialize state vector and state covariance matrix: $\hat{\mathbf{x}}_0^-$ and \mathbf{P}_0^-

2. Compute Kalman gain matrix from state covariance and estimated measurement covariance:

$$\mathbf{K}_k = \mathbf{P}_k^- \mathbf{H}_k^T [\mathbf{H}_k \mathbf{P}_k^- \mathbf{H}_k + \mathbf{R}_k]^{-1} \quad (5)$$

3. Multiply prediction error vector by Kalman gain matrix to get state correction vector and update state vector:

$$\hat{\mathbf{x}}_k = \hat{\mathbf{x}}_k^- + \mathbf{K}_k [\mathbf{z}_k - \mathbf{h}_k(\hat{\mathbf{x}}_k^-)] \quad (6)$$

4. Update error covariance

$$\mathbf{P}_k = [\mathbf{I} - \mathbf{K}_k \mathbf{H}_k] \mathbf{P}_k^- \quad (7)$$

5. Predict new state vector and state covariance matrix

$$\hat{\mathbf{x}}_k^- = \mathbf{f}_{k-1}(\hat{\mathbf{x}}_{k-1}^-) \quad (8)$$

$$\mathbf{P}_{k+1}^- = \mathbf{\Phi}_k \mathbf{P}_k \mathbf{\Phi}_k^T + \mathbf{Q}_k \quad (9)$$

where the linear approximation equations for system and measurement matrices are obtained through the relations

$$\mathbf{\Phi}_k \approx \left. \frac{\partial \mathbf{f}_k}{\partial \mathbf{x}} \right|_{\mathbf{x}=\hat{\mathbf{x}}_k^-}; \quad \mathbf{H}_k \approx \left. \frac{\partial \mathbf{h}_k}{\partial \mathbf{x}} \right|_{\mathbf{x}=\hat{\mathbf{x}}_k^-} \quad (10)$$

Equations (5–7) are the measurement update equations, and Eqs. (8) and (9) are the time update equations of the algorithm from k to step $k + 1$. These equations incorporate a measurement value into a priori estimation to obtain an improved a posteriori estimation. In the above equations, \mathbf{P}_k is the error covariance matrix defined by $E[(\mathbf{x}_k - \hat{\mathbf{x}}_k)(\mathbf{x}_k - \hat{\mathbf{x}}_k)^T]$, in which $\hat{\mathbf{x}}_k$ is an estimation of the system state vector \mathbf{x}_k , and the weighting matrix \mathbf{K}_k is generally referred to as the Kalman gain matrix. The Kalman filter algorithm starts with an initial condition value, $\hat{\mathbf{x}}_0^-$ and \mathbf{P}_0^- . When new measurement \mathbf{z}_k becomes available with the progression of time, the estimation of states and the corresponding error covariance would follow recursively ad infinity. Further detailed discussion can be referred to Brown and Hwang (1997), Farrell and Barth (1999) and Gelb (1974).

The unscented Kalman filter

In the EKF, the state distribution is approximated by a Gaussian random variable (GRV), which is then propagated analytically through the first-order linearization of the nonlinear system. Wan and van der Merwe (2000) pointed out that this will introduce large errors in the true posterior mean and covariance of the transformed GRV and lead to sub-optimal performance and sometimes filter divergence. The unscented Kalman filter (UKF) was first proposed by Julier et al. (1995) to address nonlinear state estimation in the context of control theory. The UKF addresses this problem by using a deterministic sampling approach. The

state distribution is also approximated by a GRV, but is represented using a minimal set of sample points. These sample points are carefully chosen so as to completely capture the true mean and covariance of the GRV. When the sample points are propagated through the true nonlinear system, the posterior mean and covariance can be captured accurately to the third-order of Taylor series expansion for any nonlinear system. One of the remarkable merits is that the overall computational complexity of the UKF is the same as that of the EKF (Wan and van der Merwe 2000).

Unscented transformation

The first step in the UKF is to sample the prior state distribution, i.e., generate the sigma points through the unscented transformation (UT) (Julier et al. 2000; Julier and Uhlmann 2002; Julier 2002). The unscented transform is a method for calculating the statistics of a random variable which undergoes a nonlinear transformation. The basic premise is that to approximate a probability distribution is easier than to approximate an arbitrary nonlinear transformation. A set of weighted samples or sigma points are deterministically chosen so that they completely capture the true mean and covariance of the random variable. The samples are propagated through true nonlinear equations, and the linearization of the model is not necessary.

Suppose the mean $\bar{\mathbf{x}}$ and covariance \mathbf{P} of vector \mathbf{x} are known, a set of deterministic vector called sigma points can then be found. The ensemble mean and covariance of the sigma points are equal to $\bar{\mathbf{x}}$ and \mathbf{P} . The nonlinear function $\mathbf{y} = f(\mathbf{x})$ is applied to each deterministic vector to obtain transformed vectors. The ensemble mean and covariance of the transformed vectors will give a good estimate of the true mean and covariance of \mathbf{y} , which is the key to the unscented transformation. Figure 1 illustrates the mapping of the UKF versus that of the EKF, through the transformation of: (1) the nonlinear function $\mathbf{f}(\cdot)$, shown on the top portion of the figure, and (2) its Jacobian/Hessian \mathbf{F} , shown at the bottom portion of the figure. The dot-line ellipse represents the true covariance; the solid-line ellipse represents the calculated covariance. The UKF approach estimates are expected to be closer to the true values than the EKF approach.

Consider an n dimensional random variable \mathbf{x} , having the mean $\hat{\mathbf{x}}$ and covariance \mathbf{P} , and suppose that it propagates through an arbitrary nonlinear function \mathbf{f} . The unscented transform creates $2n + 1$ sigma vectors \mathbf{X} (a capital letter) and weighted points W , given by

$$\mathbf{X}_{(0)} = \hat{\mathbf{x}} \quad (11)$$

$$\mathbf{X}_{(i)} = \hat{\mathbf{x}} + (\sqrt{(n + \lambda)\mathbf{P}})_i^T, \quad i = 1, \dots, n \quad (12)$$

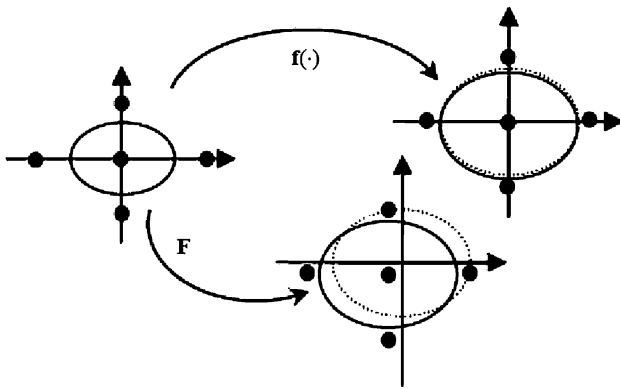


Fig. 1 Illustration of properties of UKF and EKF (Li et al. 2006)

$$\mathbf{X}_{(i+n)} = \hat{\mathbf{x}} - (\sqrt{(n + \lambda)\mathbf{P}})_i^T, \quad i = 1, \dots, n \tag{13}$$

$$W_0^{(m)} = \frac{\lambda}{(n + \lambda)} \tag{14}$$

$$W_0^{(c)} = W_0^{(m)} + (1 - \alpha^2 + \beta) \tag{15}$$

$$W_i^{(m)} = W_i^{(c)} = \frac{1}{2(n + \lambda)}, \quad i = 1, \dots, 2n \tag{16}$$

where $(\sqrt{(n + \lambda)\mathbf{P}})_i$ is the i th row (or column) of the matrix square root. $\sqrt{(n + \lambda)\mathbf{P}}$ can be obtained from the lower-triangular matrix of the Cholesky factorization; $\lambda = \alpha^2 (n + k) - n$ is a scaling parameter; α determines the spread of the sigma points around $\hat{\mathbf{x}}$ and is usually set to a small positive (e.g., $1e - 4 \leq \alpha \leq 1$); k is a second scaling parameter (usually set as 0); β is used to incorporate prior knowledge of the distribution of $\hat{\mathbf{x}}$ (When \mathbf{x} is normally distributed, $\beta = 2$ is an optimal value); $W_i^{(m)}$ is the weight for the mean associated with the i th point; and $W_i^{(c)}$ is the weigh for the covariance associated with the i th point.

The sigma vectors are propagated through the nonlinear function to yield a set of transformed sigma points,

$$\mathbf{y}_i = f(\mathbf{X}_i) \quad i = 0, \dots, 2n \tag{17}$$

The mean and covariance of \mathbf{y}_i are approximated by a weighted average mean and covariance of the transformed sigma points as follows:

$$\bar{\mathbf{y}}_u = \sum_{i=0}^{2n} W_i^{(m)} \mathbf{y}_i \tag{18}$$

$$\bar{\mathbf{P}}_u = \sum_{i=0}^{2n} W_i^{(c)} (\mathbf{y}_i - \bar{\mathbf{y}}_u)(\mathbf{y}_i - \bar{\mathbf{y}}_u)^T \tag{19}$$

As compared to the EKF’s linear approximation, the unscented transformation is accurate to the second-order for any nonlinear function.

The unscented Kalman filter

The basic premise behind the UKF is it is easier to approximate a Gaussian distribution than it is to approximate an arbitrary nonlinear function. Instead of linearizing using Jacobian matrices as in the EKF and achieving first-order accuracy, the UKF uses a deterministic sampling approach to capture the mean and covariance estimates with a minimal set of sample points. A high level of operation of the UKF is shown in Fig. 2.

To look at the detailed algorithm of the UKF, first, the set of sigma points are created by Eqs. (12) and (13). After the sigma points are generated, the time update (prediction step) of the UKF includes the following steps:

$$(\zeta_k^-)_i = f((\mathbf{X}_k^-)_i), \quad i = 0, \dots, 2n \tag{20}$$

$$\hat{\mathbf{x}}_k^- = \sum_{i=0}^{2n} W_i^{(m)} (\zeta_k^-)_i \tag{21}$$

$$\mathbf{P}_k^- = \sum_{i=0}^{2n} W_i^{(c)} [(\zeta_k^-)_i - \hat{\mathbf{x}}_k^-][(\zeta_k^-)_i - \hat{\mathbf{x}}_k^-]^T + \mathbf{Q}_k \tag{22}$$

$$(\mathbf{Z}_k^-)_i = \mathbf{h}((\zeta_k^-)_i) \tag{23}$$

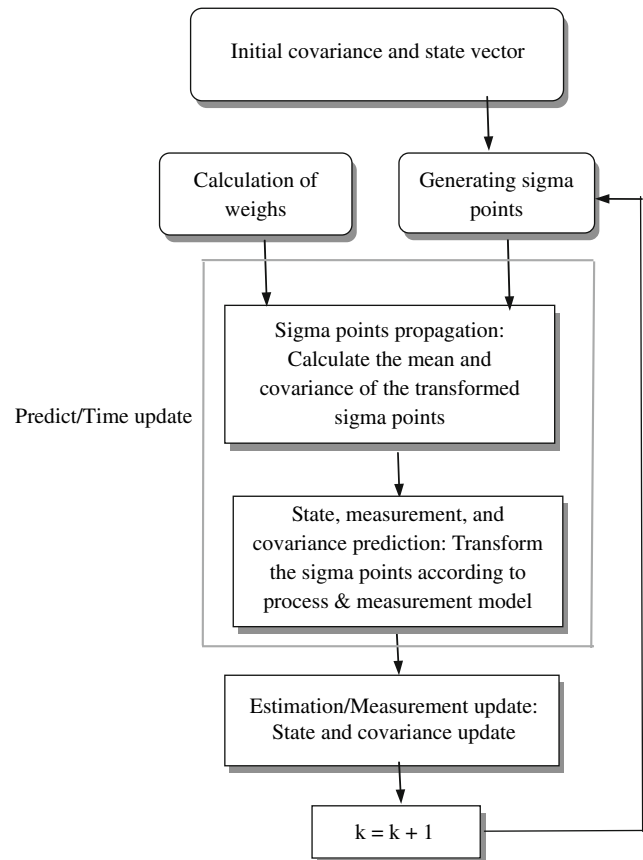


Fig. 2 High level of operation of the unscented Kalman filter

$$\hat{\mathbf{z}}_k^- = \sum_{i=0}^{2n} W_i^{(m)} (\mathbf{Z}_k^-)_i \tag{24}$$

The measurement update (correction) step of the UKF involves the following steps:

$$\mathbf{P}_{yy} = \sum_{i=0}^{2n} W_i^{(c)} [(\mathbf{Z}_k^-)_i - \hat{\mathbf{z}}_k^-][(\mathbf{Z}_k^-)_i - \hat{\mathbf{z}}_k^-]^T + \mathbf{R}_k \tag{25}$$

$$\mathbf{P}_{xz} = \sum_{i=0}^{2n} W_i^{(c)} [(\zeta_k^-)_i - \hat{\mathbf{x}}_k^-][(\mathbf{Z}_k^-)_i - \hat{\mathbf{z}}_k^-]^T \tag{26}$$

$$\mathbf{K}_k = \mathbf{P}_{xz} \mathbf{P}_{yy}^{-1} \tag{27}$$

$$\hat{\mathbf{x}}_k = \hat{\mathbf{x}}_k^- + \mathbf{K}_k (\mathbf{z}_k - \hat{\mathbf{z}}_k^-) \tag{28}$$

$$\mathbf{P}_k = \mathbf{P}_k^- - \mathbf{K}_k \mathbf{P}_{yy} \mathbf{K}_k^T \tag{29}$$

The flow chart for the UKF approach is summarized in Fig. 3. The samples are propagated through true nonlinear equations; the linearization is unnecessary (Calculation of Jacobian is not required). They can capture the states up to at least second order, where as the EKF is only a first order approximation.

Nonlinear dynamic modeling

In actual GPS navigation filter designs, there exist model uncertainties which cannot be expressed by the linear state-space model. The commonly used position-velocity (PV) model is a linear model, which is popular due to its simplicity. The linear model increases modeling errors since the actual vehicle motions are nonlinear process. It is very often the case that little a priori knowledge is available concerning the maneuver. In the modeling strategy, it has been very common that additional fictitious process noise can be added to the system model. However, the best cure for non convergence caused by unmodeled states is to correct the model. Derivation of a better, nonlinear, dynamic model is necessary for improving the estimation accuracy.

The PV model

The dynamic process of the GPS receiver in lower dynamic environment can be represented by the PV model (Brown and Hwang 1997; Farrell and Barth 1999). In such case, the GPS navigation filter includes three position states, three velocity states, and two clock states, so that the state to be estimated is a 8×1 vector. When selecting Kalman filtering as the navigation state estimator in the GPS receiver, using b and d to represent the GPS receiver clock bias and

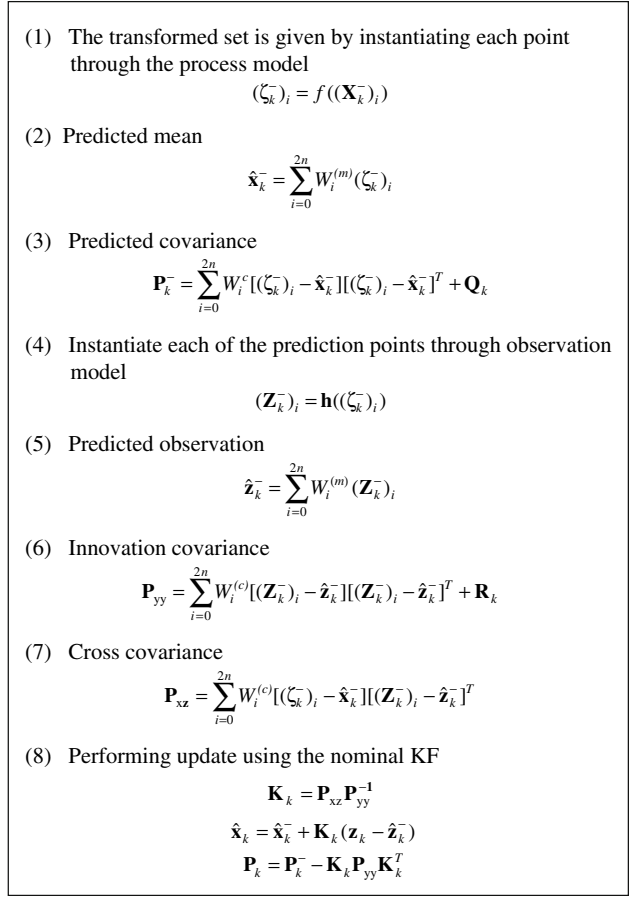


Fig. 3 Flow chart for the unscented Kalman filter

drift, the differential equation for the clock error is written as

$$\begin{aligned} \dot{b} &= d + u_b \\ \dot{d} &= u_d \end{aligned} \tag{30}$$

where $u_b \sim N(0, S_p)$ and $u_d \sim N(0, S_g)$ are independent Gaussian distributed white sequences. The PV process model governed by Eq. (1a) leads to

$$\begin{bmatrix} \dot{x}_1 \\ \dot{x}_2 \\ \dot{x}_3 \\ \dot{x}_4 \\ \dot{x}_5 \\ \dot{x}_6 \\ \dot{x}_7 \\ \dot{x}_8 \end{bmatrix} = \begin{bmatrix} 0 & 1 & 0 & 0 & 0 & 0 & 0 & 0 \\ 0 & 0 & 0 & 0 & 0 & 0 & 0 & 0 \\ 0 & 0 & 0 & 1 & 0 & 0 & 0 & 0 \\ 0 & 0 & 0 & 0 & 0 & 0 & 0 & 0 \\ 0 & 0 & 0 & 0 & 0 & 1 & 0 & 0 \\ 0 & 0 & 0 & 0 & 0 & 0 & 0 & 0 \\ 0 & 0 & 0 & 0 & 0 & 0 & 0 & 1 \\ 0 & 0 & 0 & 0 & 0 & 0 & 0 & 0 \end{bmatrix} \begin{bmatrix} x_1 \\ x_2 \\ x_3 \\ x_4 \\ x_5 \\ x_6 \\ x_7 \\ x_8 \end{bmatrix} + \begin{bmatrix} 0 \\ u_2 \\ 0 \\ u_4 \\ 0 \\ u_6 \\ u_7 \\ u_8 \end{bmatrix}$$

where x_1, x_3, x_5 represent the position components; x_2, x_4, x_6 represent the velocity components; and x_7 and x_8 represent the receiver clock offset and drift errors, respectively. These states can be implemented in the WGS-84 coordinates. Note that the state vector represented in the east, north, and altitude coordinate system is also accessible. In such case, the

coordinate transformation from WGS-84 to ENU frame for the GPS satellite positions needs to be conducted to ensure that the correct measurement information is used.

When the PV model is employed, the corresponding state transition matrix for the model can be obtained to be

$$\Phi_k = \begin{bmatrix} 1 & \Delta t & 0 & 0 & 0 & 0 & 0 & 0 \\ 0 & 1 & 0 & 0 & 0 & 0 & 0 & 0 \\ 0 & 0 & 1 & \Delta t & 0 & 0 & 0 & 0 \\ 0 & 0 & 0 & 1 & 0 & 0 & 0 & 0 \\ 0 & 0 & 0 & 0 & 1 & \Delta t & 0 & 0 \\ 0 & 0 & 0 & 0 & 0 & 1 & 0 & 0 \\ 0 & 0 & 0 & 0 & 0 & 0 & 1 & \Delta t \\ 0 & 0 & 0 & 0 & 0 & 0 & 0 & 1 \end{bmatrix} \quad (31)$$

The process noise covariance matrix for the PV model is:

$$Q_k = \begin{bmatrix} Q_x & & & & & & & \\ & Q_y & & & & & & \\ & & Q_z & & & & & \\ & & & S_f \Delta t + S_g \frac{\Delta t^3}{3} & & & & \\ & & & S_g \frac{\Delta t^2}{2} & & S_g \frac{\Delta t^2}{2} & & \\ & & & & & & S_g \Delta t & \end{bmatrix} \quad (32)$$

where the submatrices are given by

$$Q_x = Q_y = Q_z = \begin{bmatrix} S_p \frac{\Delta t^3}{3} & S_p \frac{\Delta t^2}{2} \\ S_p \frac{\Delta t^2}{2} & S_p \Delta t \end{bmatrix}$$

The states and the measurements are related nonlinearly. The nonlinear pseudorange equation can be linearized by expanding Taylor’s series around the approximate (or nominal) user position $(\hat{x}_n, \hat{y}_n, \hat{z}_n)$ and neglecting the higher terms. If only the pseudorange observables are available, the linearized measurement equation based on n observables can be written as given by:

$$\begin{bmatrix} \rho_1 \\ \rho_2 \\ \vdots \\ \rho_n \end{bmatrix} = \begin{bmatrix} \hat{\rho}_1 \\ \hat{\rho}_2 \\ \vdots \\ \hat{\rho}_n \end{bmatrix} + \begin{bmatrix} h_x^{(1)} & 0 & h_y^{(1)} & 0 & h_z^{(1)} & 0 & 1 & 0 \\ h_x^{(2)} & 0 & h_y^{(2)} & 0 & h_z^{(2)} & 0 & 1 & 0 \\ \vdots & \vdots & \vdots & \vdots & \vdots & \vdots & \vdots & \vdots \\ h_x^{(n)} & 0 & h_y^{(n)} & 0 & h_z^{(n)} & 0 & 1 & 0 \end{bmatrix} \begin{bmatrix} x_1 \\ x_2 \\ x_3 \\ x_4 \\ x_5 \\ x_6 \\ x_7 \\ x_8 \end{bmatrix} + \begin{bmatrix} v_{\rho_1} \\ v_{\rho_2} \\ \vdots \\ v_{\rho_n} \end{bmatrix} \quad (33)$$

where the elements of the measurement model \mathbf{H}_k are the partial derivatives of the predicted measurements with respect to each state, which is an $(n \times 8)$ matrix.

$$\mathbf{H}_k = \frac{\partial \mathbf{h}_k}{\partial \mathbf{x}} = \begin{bmatrix} h_x^{(1)} & 0 & h_y^{(1)} & 0 & h_z^{(1)} & 0 & 1 & 0 \\ h_x^{(2)} & 0 & h_y^{(2)} & 0 & h_z^{(2)} & 0 & 1 & 0 \\ \vdots & \vdots & \vdots & \vdots & \vdots & \vdots & \vdots & \vdots \\ h_x^{(n)} & 0 & h_y^{(n)} & 0 & h_z^{(n)} & 0 & 1 & 0 \end{bmatrix} \quad (34)$$

The norm of the expected pseudorange $\mathbf{h}_k(\hat{\mathbf{x}}_k^-)$ based on the GPS satellite position and the *a priori* state estimate $\hat{\mathbf{x}}_k^-$ is given by

$$\hat{r}_i = \|\mathbf{h}_k(\hat{\mathbf{x}}_k^-)\| = \sqrt{(\hat{x}_k^- - x_i)^2 + (\hat{y}_k^- - y_i)^2 + (\hat{z}_k^- - z_i)^2}$$

The vector $(h_x^{(i)}, h_y^{(i)}, h_z^{(i)})$, $i = 1, \dots, n$, denotes the line-of-sight vector from the user to the satellites:

$$h_x^{(i)} = \frac{\hat{x}_k^- - x_i}{\hat{r}_i}; \quad h_y^{(i)} = \frac{\hat{y}_k^- - y_i}{\hat{r}_i}; \quad h_z^{(i)} = \frac{\hat{z}_k^- - z_i}{\hat{r}_i} \quad (35)$$

Assuming measurement errors among satellites are uncorrelated, we have

$$\mathbf{R}_k = \begin{bmatrix} r_{\rho_1} & & & & & & & \mathbf{0} \\ & r_{\rho_2} & & & & & & \\ & & \ddots & & & & & \\ \mathbf{0} & & & & & & & r_{\rho_n} \end{bmatrix} \quad (36)$$

The proposed nonlinear model

Although it has been very common that additional fictitious process noise can be added to the system model, however, the best cure for non convergence caused by unmodeled states is to correct the model.

To construct the nonlinear dynamic model, consider a vehicle moving at the velocity represented as $\mathbf{V}_b = u_b \vec{i} + v_b \vec{j} + w_b \vec{k}$. The velocity in the fixed frame in terms of Euler angles and body velocity components has the relation

$$\mathbf{V} = \begin{bmatrix} \dot{x} \\ \dot{y} \\ \dot{z} \end{bmatrix} = \begin{bmatrix} C_\theta C_\psi & S_\Phi S_\theta C_\psi - C_\Phi S_\psi & C_\Phi S_\theta C_\psi + S_\Phi S_\psi \\ C_\theta S_\psi & S_\Phi S_\theta S_\psi + C_\Phi C_\psi & C_\Phi S_\theta S_\psi - S_\Phi C_\psi \\ -S_\theta & S_\Phi C_\theta & C_\Phi C_\theta \end{bmatrix} \begin{bmatrix} u_b \\ v_b \\ w_b \end{bmatrix}$$

where the following notations are used: $S_\Phi \equiv \sin(\Phi)$, $C_\Phi \equiv \cos(\Phi)$, $S_\theta \equiv \sin(\theta)$, $C_\theta \equiv \cos(\theta)$, $S_\psi \equiv \sin(\psi)$, and $C_\psi \equiv \cos(\psi)$. Based on the idea, the dynamic process model of the GPS receiver can be represented by the nonlinear model.

$$\begin{aligned} \dot{x} &= u_b \cos \theta \cos \psi + v_b (\sin \Phi \sin \theta \cos \psi - \cos \Phi \sin \psi) \\ &\quad + w_b (\cos \Phi \sin \theta \cos \psi + \sin \Phi \sin \psi) \\ \dot{y} &= u_b \cos \theta \sin \psi + v_b (\sin \Phi \sin \theta \sin \psi + \cos \Phi \cos \psi) \\ &\quad + w_b (\cos \Phi \sin \theta \sin \psi - \sin \Phi \cos \psi) \\ \dot{z} &= -u_b \sin \theta + v_b \sin \Phi \cos \theta + w_b \cos \Phi \cos \theta \end{aligned} \quad (37)$$

Suppose that, as the nonholonomic constraint, only the longitudinal movement is considered and the lateral slippage is neglected. In case the velocity in the *x*-component of body frame is considered, $\|\mathbf{V}_b\| \approx \|u_b \vec{i}\| \approx V$, the model can be simplified

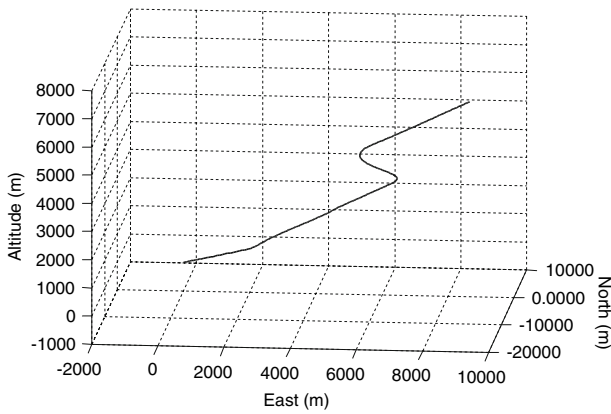


Fig. 4 Three dimensional vehicle trajectory (in ENU frame)

Since we assumed that the differential GPS (DGPS) mode is used most of the errors can be corrected, but the multipath and receiver measurement thermal noise cannot be eliminated. The measurement noise variances r_{ρ_i} value are assumed a priori known, which is set to be $(3.5 \text{ m})^2$. Let each of the white-noise spectral amplitudes that drive the random walk position states be $S_p = 0.1 \text{ m}^2/(\text{rad}\cdot\text{s})$. Also, let the clock model spectral amplitudes be $S_f = 0.4 \times 10^{-18} \text{ s}$ and $S_g = 1.58 \times 10^{-18} \text{ s}^{-1}$. These spectral amplitudes can be used to find the \mathbf{Q}_k parameters in Eq. (32) for the PV model. The measurement noise covariance matrix is

$$\mathbf{R}_k = \begin{bmatrix} 15 & & & \mathbf{0} \\ & 15 & & \\ & & \ddots & \\ \mathbf{0} & & & 15 \end{bmatrix}$$

The sigma points capture the same mean and covariance irrespective of the choice of matrix square root which is used. The numerical efficient and stable method such as the Cholesky factorization has been used in obtaining the sigma points.

Table 1 Description of vehicle motion

Time interval (s)	Motion
0–50	Constant velocity
51–100	Constant acceleration
101–150	Constant velocity
151–200	Variable acceleration
201–250	Constant velocity
251–350	Circular motion, clockwise turn
351–450	Constant velocity

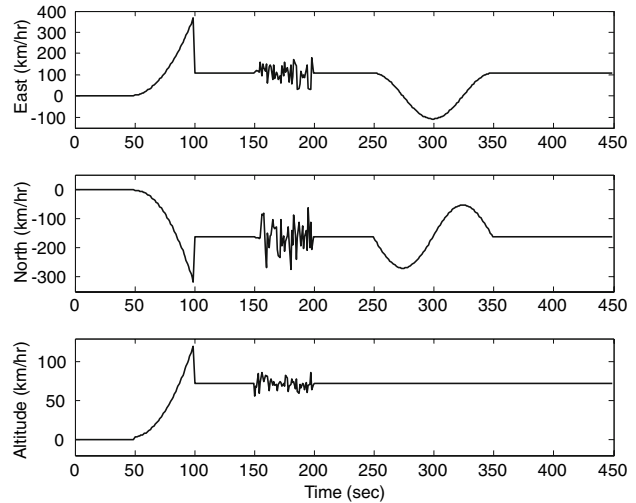


Fig. 5 Vehicle velocity in the east, north, and vertical components

Results based on the PV model

The parameters for the UKF are: $\alpha = 0.1, \beta = 2, \gamma = 0$. Figures 7 and 8 provide comparison of GPS positioning errors for EKF and UKF when the PV model is utilized. In the three time intervals, 51–100, 151–200, 251–350 s, the vehicle is conducting maneuvering, and the mismatch of the model leads to large navigation error. It is seen that results from both methods almost overlap each other and little benefit was gained based on the UKF. In order to improve the navigation estimation accuracy, utilization of a nonlinear model for better description on the vehicle dynamic will be more plausible to achieve better estimation accuracy.

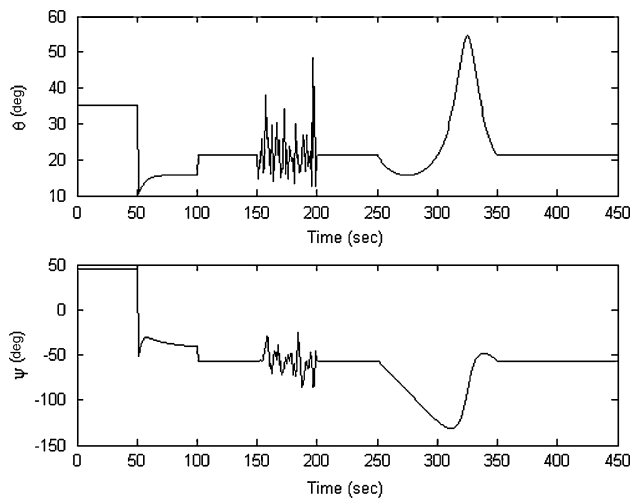


Fig. 6 Pitch and heading angle parameters of the vehicle for the simulation scenario

Results based on the nonlinear model

For comparison purpose, the same values of process noise covariance parameters will be utilized for both the EKF and UKF. Two cases are implemented: (1) a smaller process noise is used: $q_{ii} = 0.02, i = 1, \dots, 7$, for which case $\alpha = 1e - 4, \beta = 2, \gamma = 0$; (2) a larger process noise is used: $q_{ii} = 3, i = 1, \dots, 7$, for which case $\alpha = 0.007, \beta = 2, \gamma = 0$.

Global positioning system navigation performance comparison between EKF and UKF, when the proposed nonlinear model is utilized are given in Figs. 9, 10, 11, 12, 13 and 14. Figures 9, 11 and 10, 12 show the east, north and vertical components of navigational errors for the EKF

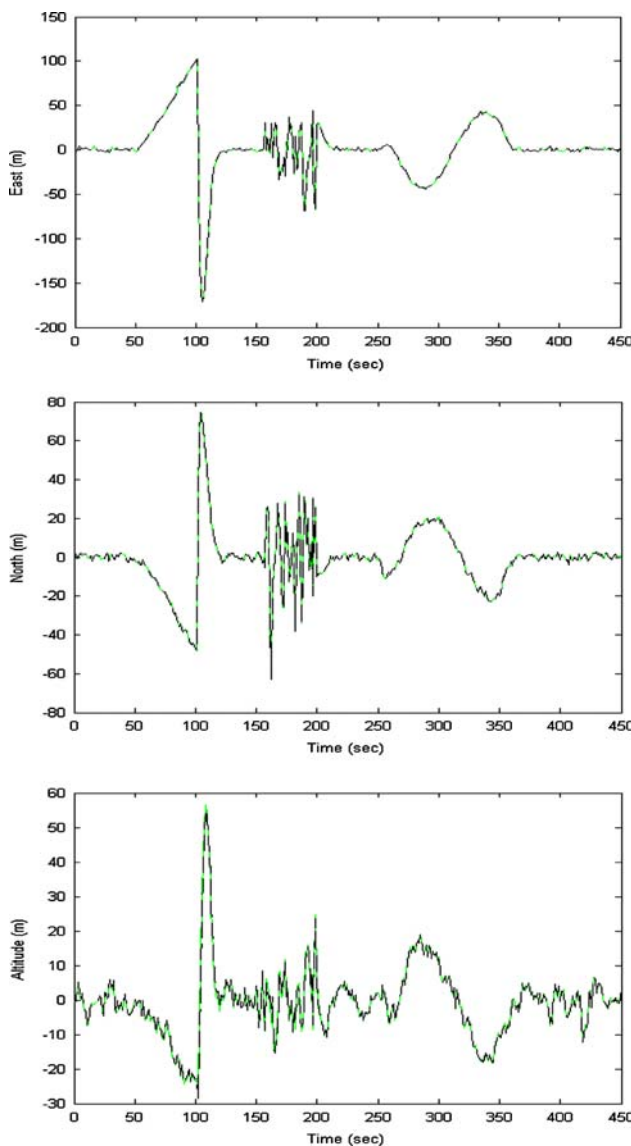


Fig. 7 Comparison of GPS positioning errors for EKF and UKF when the PV model is used (note that both results almost overlap each other)

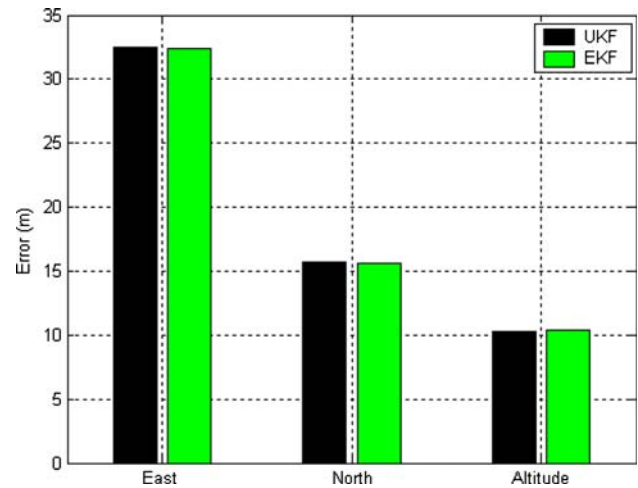


Fig. 8 Comparison of RMSE when the conventional PV model is utilized

and the UKF, for smaller and larger process noise covariance, respectively. It can be seen that substantial estimation accuracy improvement is obtained by using the proposed strategy, discussed as follows:

1. In the four time intervals, 0–50, 101–150, 201–250, 351–450 s, the vehicle is not maneuvering and is conducting constant-velocity straight-line motion for all the three components. For this case, with good system modeling, therefore both the EKF and UKF provide good results. The navigation accuracies based on the two approaches have relatively smaller difference.
2. In the three time intervals, 51–100, 151–200, 251–350 s, the vehicle is conducting maneuvering. The significant mismatch of the model leads the large errors in the conventional EKF solution. The UKF with nonlinear model that better describes the vehicle dynamics is more able to achieve better navigation accuracy.

The three velocity components, longitudinal velocity, and attitude angles of the vehicle can be estimated from the GPS filter as part of the state variables. Figures 13 and 14 provide the comparison of velocity errors and the Euler angle errors for EKF and UKF approaches, respectively. Velocity accuracies determined by both filters are equivalent. In certain time epochs, large estimation errors are induced, due to large changes in velocity. Certainly, introducing very large process noise will improve the accuracy in these epochs, accompanied by the serious degradation of velocity estimation accuracy in the remaining low dynamic regions. Estimation accuracies for attitude angles are about the same order except that UKF has better smoothness and shorter transition time.

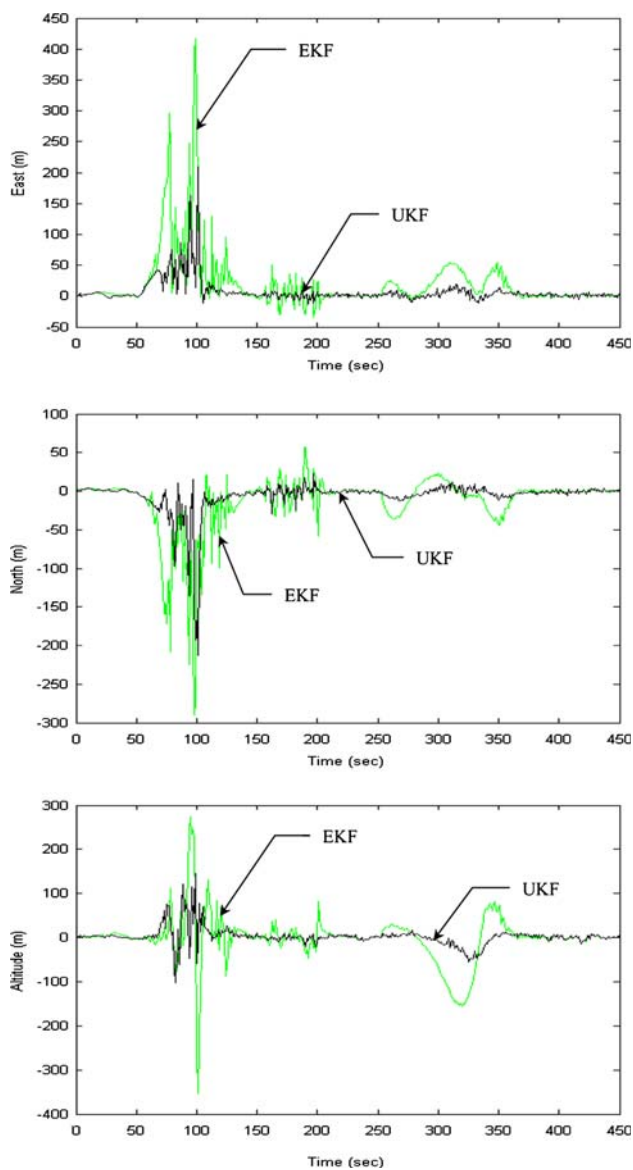


Fig. 9 Comparison of GPS positioning errors for EKF and UKF when the proposed nonlinear model is used (smaller process noise covariance has been used)

Conclusions

In light of UKF's superiority to extended Kalman filter, this paper has presented an unscented Kalman filtering approach for GPS navigation processing. In the proposed estimation mechanism, a nonlinear dynamic model has been suggested. The nonlinear model has been demonstrated to be effective in navigation accuracy improvement. The reason is due to the fact that the UKF is able to deal with the nonlinear formulation, while the linear model does not reflect the actual dynamic behavior when the vehicle is maneuvering. Therefore, in the case that PV model is employed as the dynamic process model, the performance

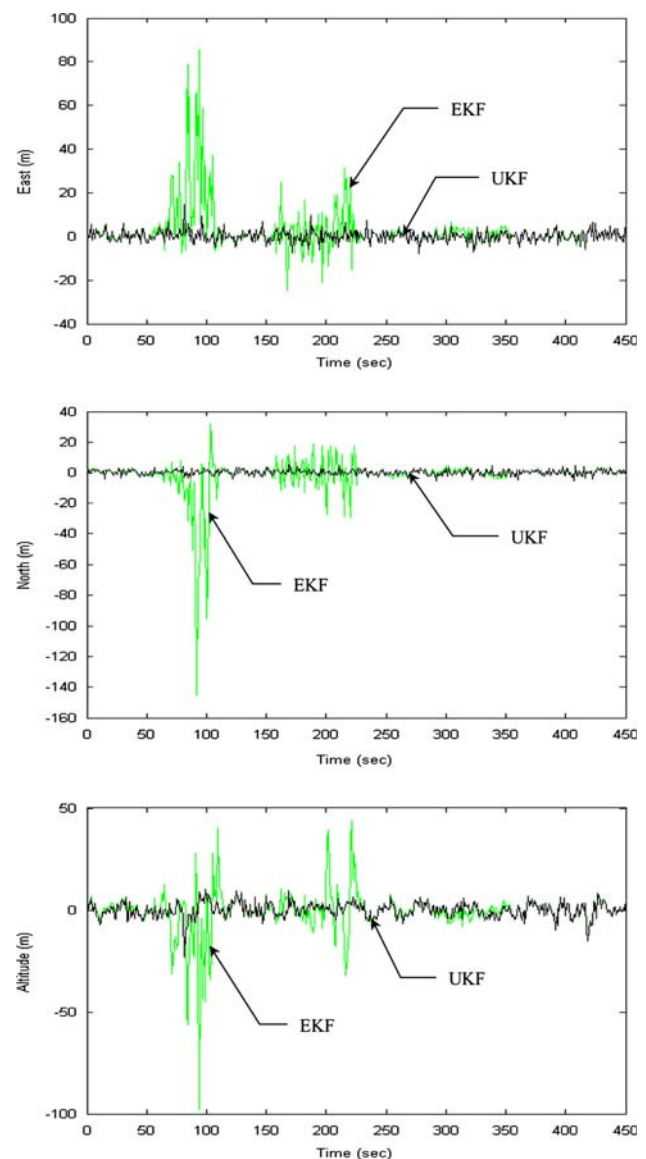


Fig. 10 Comparison of GPS positioning errors for EKF and UKF when the proposed nonlinear dynamic model is used (larger process noise covariance has been used)

improvement from the UKF will not be obtained. The UKF with nonlinear model will ensure better description on the vehicle dynamics and will be able to achieve better navigation accuracy. Navigation accuracy based on the proposed method has been compared to that of the conventional EKF approach and has demonstrated substantial navigational accuracy improvement. Tuning of parameters for the UKF and process noise covariance should be considered; more completed dynamic model which better describes the vehicle dynamic model can be conducted in future work. In additions, the adaptive algorithm has been one of the approaches to prevent divergence problem when precise knowledge on the system models are not available.

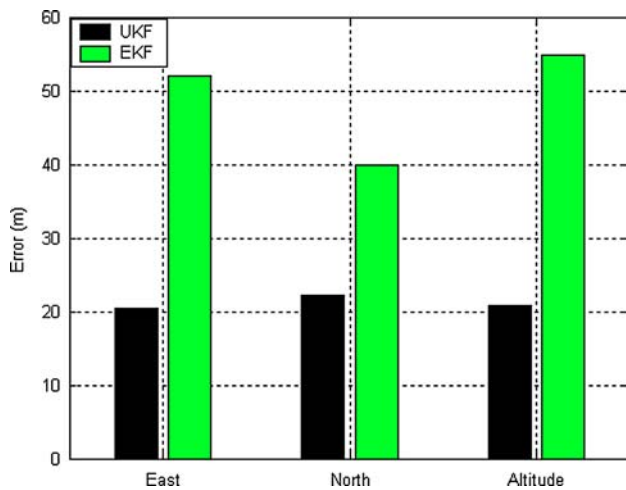


Fig. 11 Comparison of RMSE when the proposed nonlinear dynamic model with smaller noise covariance is used

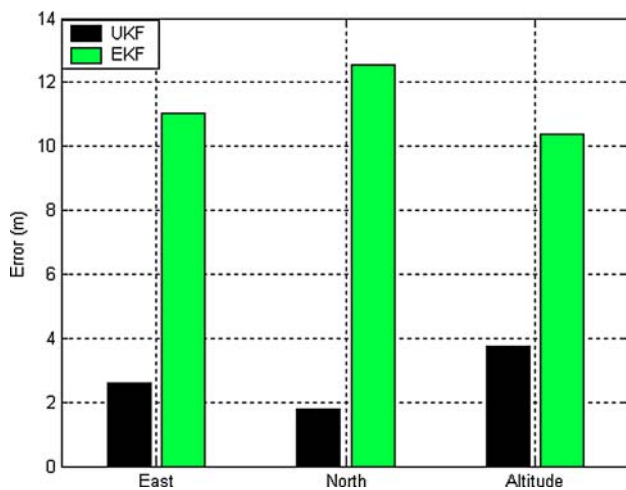


Fig. 12 Comparison of RMSE when the proposed nonlinear dynamic model with larger noise covariance is used

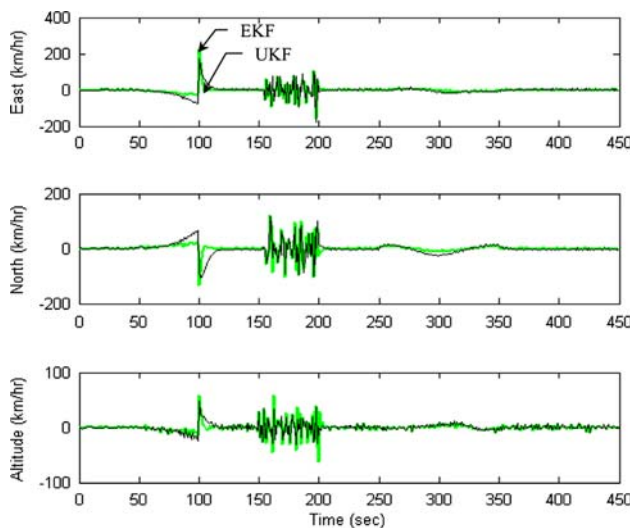


Fig. 13 Comparison of velocity errors for EKF and UKF approaches

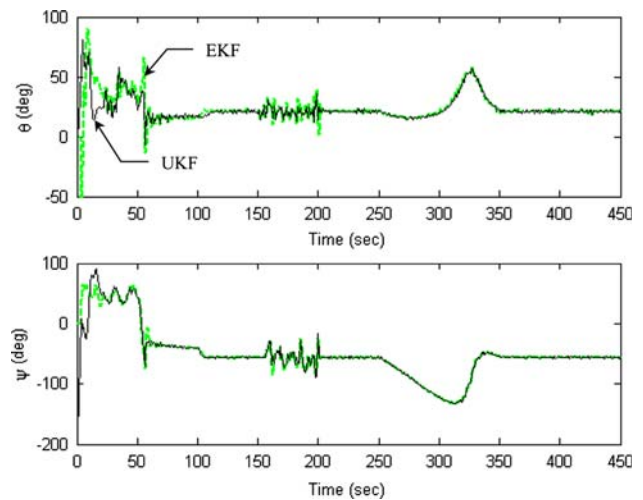


Fig. 14 Comparison of Euler angle errors for EKF and UKF approaches

These adaptive approaches used in the standard EKF can also be incorporated for tuning the noise covariance matrices based on dynamically adjusting the parameters, leading to the adaptive unscented Kalman filter (AUKF) for further improvement.

Acknowledgments Funding for this work was provided by the National Science Council of the Republic of China under grant numbers NSC 95-2221-E-019-026 and NSC 96-2221-E-019-007. The authors gratefully acknowledge the support. Efforts made by Shih-Yao Lai and Guo-Sheng Shieh on simulation implementation for the revised version are also gratefully acknowledged.

References

Brown R, Hwang PYC (1997) Introduction to random signals and applied Kalman filtering. Wiley, New York

Crassidis JL (2006) Sigma-point Kalman filtering for integrated GPS and inertial navigation. *IEEE Trans Aerosp Electron Syst* 42(2):750–756

Farrell JA, Barth M (1999) The global positioning system and inertial navigation. McCraw-Hill, New York

Gelb A (1974) Applied optimal estimation. MIT Press, Cambridge

Gordon N, Salmond DJ, Smith AFM (1993) Novel approach to nonlinear/non-Gaussian Bayesian state estimation. *IEE Proc-F* 140(2):107–113

Julier SJ (2002) The scaled unscented transformation. In: Proceedings of the American control conference. Anchorage, pp 4555–4559

Julier SJ, Uhlmann JK (1997) A new extension of the Kalman filter to nonlinear systems. In: Proceedings of the 11th international symposium on aerospace/defense sensing, simulation and controls, pp 54–65

Julier SJ, Uhlmann JK (2002) Reduced sigma point filters for the propagation of means and covariances through nonlinear transformations. In: Proceeding of the American control conference, pp 887–892

Julier SJ, Uhlmann JK, Durrant-whyte HF (1995) A new approach for filtering nonlinear system. In: Proceeding of the American control conference, pp 1628–1632

- Julier SJ, Uhlmann JK, Durrant-whyte HF (2000) A new method for the nonlinear transformation of means and covariances in filters and estimators. *IEEE Trans Automat Control* 5(3):477–482
- Li Y, Wang J, Rizos C, Mumford PJ, Ding W (2006) Low-cost tightly coupled GPS/INS integration based on a nonlinear Kalman filter design. In: *Proceedings of the U.S. institute of navigation national tech. meeting*, pp 958–966
- van der Merwe R, Wan EA (2004) Sigma-point Kalman filters for nonlinear estimation and sensor- fusion: applications to integrated navigation, in: *Proceedings of the AIAA guidance, navigation and control conference*
- Norgaard M, Poulsen NK, Ravn O (2000) New developments in state estimation for nonlinear systems. *Automatica* 36(11):1627–1638
- Simon D (2006) *Optimal state estimation, Kalman, H_∞, and nonlinear approaches*. Wiley, New York
- Wan EA, van der Merwe R (2000) The unscented Kalman filter for nonlinear estimation, in: *Proceedings of adaptive systems for signal processing, communication and control (AS-SPCC) symposium, Alberta*, pp 153–156
- Wan EA, van der Merwe R (2001) The unscented Kalman filter. In: Haykin S (ed) *Kalman filtering and neural networks*, chap 7. Wiley, New York